Fabrication and Characterization of a MEMS Thermal Convective Accelerometer on Silicon-in-Glass Substrate

Yizhou Ye, Shu Wan, Shen Li, Yunhao Peng, Xuefeng He, *Member, IEEE*, and Ming Qin, *Member, IEEE*

***Abstract*—In this article, the fabrication and characterization of a 2-D micro-electromechanical system (MEMS) thermal convective accelerometer are demonstrated. This sensor consists of a heater and four thermistors. The central heater warms up the chip to a temperature higher than the ambient, while the four thermistors, which are arranged symmetrically around the heater, monitor the temperature gradients induced by the acceleration. The heater and thermistors are fabricated on one side of a silicon-in-glass (SIG) substrate using a glass reflow process. The utilization of this SIG substrate not only enhances the sensor robustness at low power consumption but also allows the lead wires of the sensor to be directly soldered to the printed circuit board (PCB), significantly simplifying the sensor packaging. Experimental tests on the fabricated accelerometer indicate that the sensor can measure acceleration exceeding 80 m/s^2, with an approximate linear sensitivity of about 150 mV/g. The proposal of this SIG-based device provides a new paradigm for developing high-reliability and low-power-consumption MEMS accelerometers.**

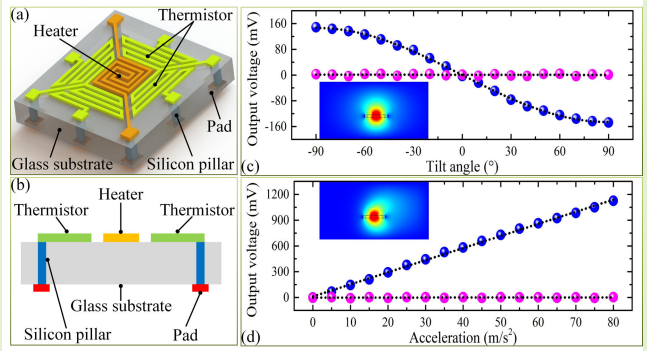

***Index Terms*— Accelerometer, micro-electromechanical systems (MEMS), glass reflow process, tilt sensor.**

I. Introduction

ACCELEROMETERS have become ubiquitous sensors, finding widespread applications in a variety of domains, such as motion sensing, vehicle stability and navigation, structural health monitoring, industrial machinery, and robotics [1], [2], [3], [4], [5]. In recent years, the rapid progress of semiconductor fabrication technology has motivated the development of micro-electromechanical systems (MEMS) accelerometers, and the devices based on capacitive [6], [7], [8], resonant [9], [10], [11], thermal convection [12], [13], [14], [15], [16], and optical [17], [18], [19] principles have already been successfully fabricated, with several commercial products currently entering the consumer electronics markets [20], [21], [22]. Among all types of MEMS accelerometers, the sensor based on thermal convection is considered an important branch due to its advantageous features, including a simple structure, high shock survivability, and easy integration with the conditioning circuit. To minimize the spurious heat shunt and reduce power consumption, the active components in this device are typically isolated from the silicon substrate by suspending the heater and thermistors on a membrane or even elevating them directly above the substrate [23], [24], [25], [26], [27]. However, the suspended structure created through either front-side or back-side silicon anisotropic etching is unable to withstand strong vibrations or mechanical shocks [28], [29]. Moreover, the thermal stress variations resulting from temperature changes also have a significant impact on the performance of the sensor [28], [30], [31].

The unreliable nature of the suspension membrane necessitates the development of a thermal accelerometer that strikes a balance between structural robustness and low power consumption. In this article, a silicon-in-glass (SIG) substrate produced through the glass reflow process is utilized

Manuscript received 3 January 2024; revised 2 February 2024; accepted 6 February 2024. Date of publication 15 February 2024; date of current version 2 April 2024. This work was supported in part by the National Natural Science Foundation of China under Grant 62104022 and in part by the Key Project of Science and Technology Research Program of Chongqing Education Commission of China under Grant kjzd-k202000105. The associate editor coordinating the review of this article and approving it for publication was Prof. Tsung-Heng Tsai. *(Corresponding authors: Yizhou Ye; Ming Qin.)*

Yizhou Ye, Shu Wan, Shen Li, and Xuefeng He are with the Key Laboratory of Optoelectronic Technology and Systems, Ministry of Education, Chongqing University, Chongqing 400044, China (e-mail: yzye@cqu.edu.cn).

Yunhao Peng is with the 26th Research Institute of China Electronics Technology Group Corporation, Chongqing 401332, China.

Ming Qin is with the Key Laboratory of MEMS of the Ministry of Education, Southeast University, Nanjing 210096, China (e-mail: mqin@seu.edu.cn).

Digital Object Identifier 10.1109/JSEN.2024.3364648

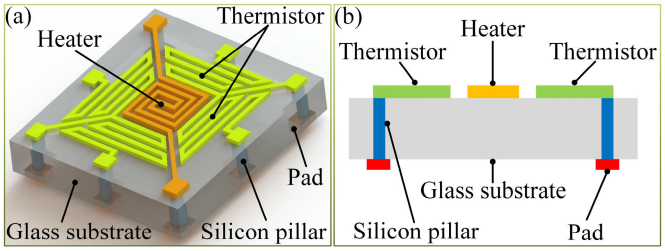

Fig. 1. (a) Perspective view and (b) cross-sectional view of the proposed MEMS thermal convective accelerometer based on SIG substrate.

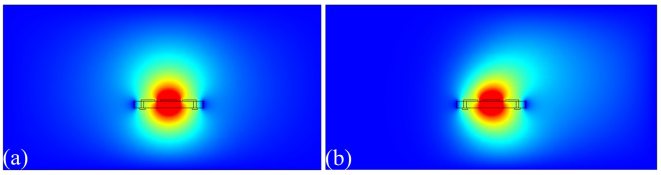

Fig. 2. Operation principle of the MEMS thermal convective accelerometer. (a) Temperature distribution on the surface of the sensor chip in the absence of acceleration. (b) Temperature distribution on the surface of the sensor chip when a leftward acceleration is applied.

to manufacture the thermal convective accelerometer [32], [33], [34]. The heater and thermistors of the thermal accelerometer are positioned on the glass substrate, while the vertical silicon through-wafer interconnects are incorporated to replace the bonding wires on the front surface of the chip. The utilization of the SIG substrate offers several benefits. First, the lower thermal conductivity of the glass substrate effectively reduces inefficient heat conduction through the substrate, leading to an enhanced energy utilization efficiency of the sensor while upholding its reliability. Second, the inclusion of silicon through-wafer interconnects on the SIG substrate allows for direct wire bonding of the sensor chip to the PCB from the backside, streamlining the sensor packaging process.

The structure of this article is as follows. Section II provides an overview of the working principle and design consideration of the MEMS thermal convective accelerometer based on the SIG substrate. Section III presents a detailed account of the fabrication process. In Section IV, we present the experimental results and engage in discussions. Finally, Section V summarizes this article in a conclusion.

II. Principle and Analysis

A. Sensor Principle

Fig. 1 depicts the structural schematic and the cross-sectional view of the proposed SIG-based thermal convective accelerometer. This sensor comprises a central heater and four thermistors symmetrically distributed around the heater. To enhance sensor reliability while maintaining low power consumption, an SIG substrate created through a glass reflow process is utilized for fabrication. By employing this substrate, the heater and thermistors are placed on the low thermal conductivity glass bulk to mitigate the impact of stress on sensor performance, commonly encountered in conventional silicon membrane structures. Moreover, the connection between the sensor and the backend processing circuity can be achieved through the silicon pillars on the SIG substrate, resulting in significant simplification of sensor integration and packaging.

The working principle of the thermal convective accelerometer is depicted in Fig. 2. In the absence of acceleration, the thermal field on the sensor surface remains symmetric, and the thermistors detect the same temperature [Fig. 2(a)]. When an acceleration is applied to the sensor, the symmetry of the temperature field on the chip surface is disrupted, causing the two opposite thermistors to detect different temperatures [Fig. 2(b)]. Therefore, by measuring the temperature difference between these two opposite thermistors, the magnitude and direction of the applied acceleration can be determined.

B. Design Consideration

For the sensors based on the thermal principle, the primary limitation is their high power consumption. Generally, the overall power dissipation P_{total} of the thermal sensor can be attributed to conductive heat transfer P_{cond} and convective heat transfer P_{conv}, with thermal radiation being negligible in most cases. Therefore, the power consumption P_{total} of the sensor can be mathematically expressed as follows:

$$P_{\text{total}} \approx P_{\text{cond}} + P_{\text{conv}}. \tag{1}$$

In the thermal convective accelerometer, when the heater is activated, the current passing through it generates Joule heat, leading to an elevation in the heater temperature. The heat is then conducted from the heater to the substrate through their contact interface. Additionally, the heat is dissipated to the surrounding air through convection. Typically, the thermal conductivity coefficient far surpasses the heat transfer coefficient for convection, resulting in predominant heat dissipation through thermal conduction. However, the operational principle of the thermal convective accelerometer requires optimizing power allocation to enhance heat exchange with the surrounding air, thereby minimizing dissipation through thermal conduction between the heater and the substrate. Therefore, in the field of thermal convective accelerometer research, many efforts have been made to reduce the sensor power consumption by mitigating the thermal conduction between the heater and the substrate. The feasible methods mainly involve arranging the heater and thermistors on the suspended membrane or even elevating them above the substrate. However, the fabricated suspended structure is unable to withstand vibration or shocks, and the thermal stress variation resulting from the temperature changes also adversely affects the performance of the sensor.

To address these issues, an SIG substrate is utilized to fabricate the thermal convective accelerometer. This substrate employs the glass with relatively low thermal conductivity, effectively limiting inefficient energy dissipation through substrate thermal conduction. Consequently, more heat is available for exchange with the surrounding airflow. According to convective heat transfer theory, when an acceleration is applied along the x-direction, the temperature difference S

between the two opposing thermistors in the x-direction is directly proportional to the Rayleigh number Ra [35], while the Rayleigh number Ra, a dimensionless quantity, represents the ratio of inertial force to viscous force and is commonly used to characterize the convection flow within the device. Therefore, the temperature difference S between the two opposing thermistors on the chip surface can be expressed by the following equation [36]:

$$S \propto \mathrm{Ra} = \frac{a\beta\Delta T L^3}{\nu^2}\frac{\mu C_p}{k} \tag{2}$$

where a represents the applied acceleration, β is the coefficient of fluid volume expansion, ΔT is the temperature difference between the heater and ambient, L is the characteristic length of the chip, and ν, μ, C_p, and k are the kinematic viscosity, dynamic viscosity, specific heat, and thermal conductivity of the fluid, respectively. This expression indicates that if the overheat temperature, characteristic length, and parameters related to the fluid properties, such as β, ν, μ, C_p, and k, remain constant regardless of temperature variations; then, the measured temperature difference S between the opposing thermistors will solely depend on the applied acceleration a. Therefore, in the thermal convective accelerometer, it is theoretically feasible to determine the acceleration by measuring the temperature difference between the opposing thermistors.

III. Fabrication

A. Fabrication

The proposed thermal convective accelerometer was fabricated using a MEMS process. The simplified fabrication process, depicted in Fig. 3, mainly involves seven steps:

1) defining silicon pillars within the silicon cavities on a highly conductive silicon wafer using deep reaction ion etching (DRIE);
2) sealing the silicon cavities with a borosilicate glass wafer through anodic bonding;
3) filling the silicon cavities with reflowed glass to create a reflowed wafer;
4) thinning and grinding the top glass layer and the bottom silicon layer to form the SIG substrate;
5) sputtering, patterning Pt, and coating a Si_3N_4 film on the front surface of the SIG substrate to form the protected heater and thermistors;
6) sputtering Au on the back surface of the substrate to create pads for electric connections;
7) scribing to remove unwanted silicon and retain the prepared accelerometer chip.

The fabrication process of the thermal convective accelerometer begins with spin-coating and patterning a thick layer of AZ4620 photoresist onto a highly conductive 4-in silicon wafer with a thickness of 500 μm. The wafer is then subjected to etching using DRIE to create cavities with a depth of 250 μm.

The next step involves anodic bonding, where a 350-μm borosilicate glass wafer is bonded onto the silicon wafer, sealing the silicon cavities. The bonded wafers undergo a furnace treatment at 900 °C for 3 h. During this process, the glass becomes viscous, and the pressure difference between the inside and outside of the cavity causes it to flow into the cavity. Cooling and annealing procedures follow.

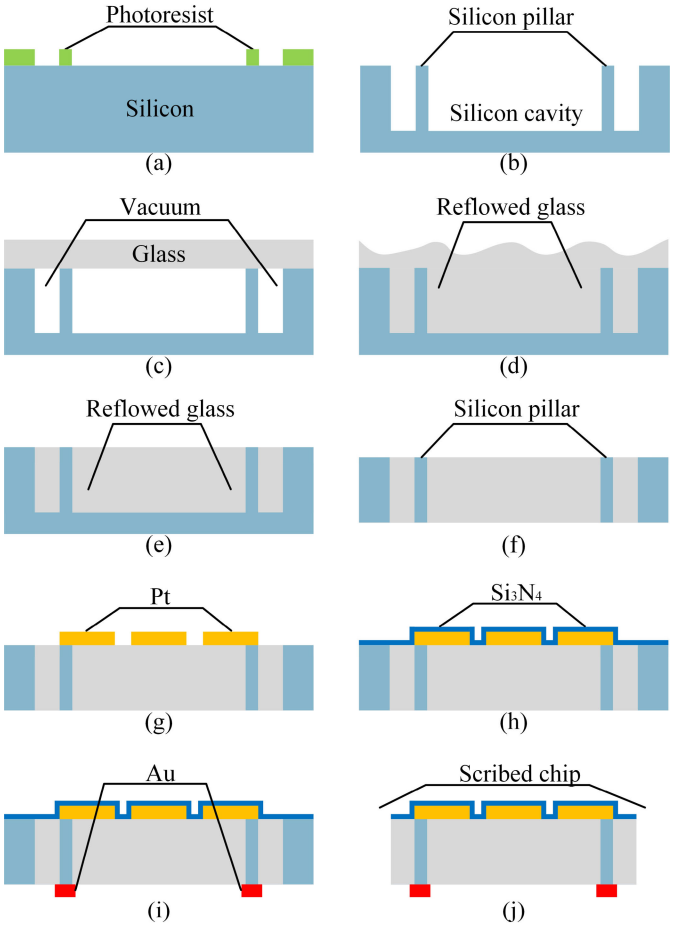

Fig. 3. Fabrication process of the MEMS thermal convective accelerometer. (a) Patterning on the silicon wafer. (b) Forming cavities and pillars on the silicon water. (c) Anodic bonding a glass wafer to the silicon wafer. (d) Reflowing glass into silicon cavities. (e) Thinning and grinding the top glass layer. (f) Removing the bottom silicon layer by thinning and grinding. (g) Sputtering and patterning Pt. (h) Depositing Si_3N_4 passivation film. (i) Sputtering Au. (j) Scribing the wafer.

Then, the SIG substrate is obtained through thinning, grinding, and chemical mechanical polishing (CMP). The top glass layer and the bottom silicon layer are removed, resulting in a final SIG substrate with an approximate thickness of 200 μm.

In the subsequent steps, a 150-nm-thick Pt layer is sputtered and patterned on the front surface of the SIG substrate using the lift-off process to create the heater and thermistors. Before Pt deposition, a 30-nm-thick Ti layer is sputtered to enhance adhesion. A 200-nm Si_3N_4 layer is then deposited using a plasma-enhanced chemical vapor deposition (PECVD) as a passivation layer for sensor protection. Finally, a 300-nm-thick Au layer is sputtered on the back surface of the SIG substrate to form the bonding pads.

Fig. 4(a) presents the photographs of the fabricated SIG-based thermal convective accelerometer, which has overall dimensions of 4 × 4 × 0.18 mm. The measured resistances of the heater and thermistors are approximately 100 Ω and 2.6 kΩ, respectively, at room temperature.

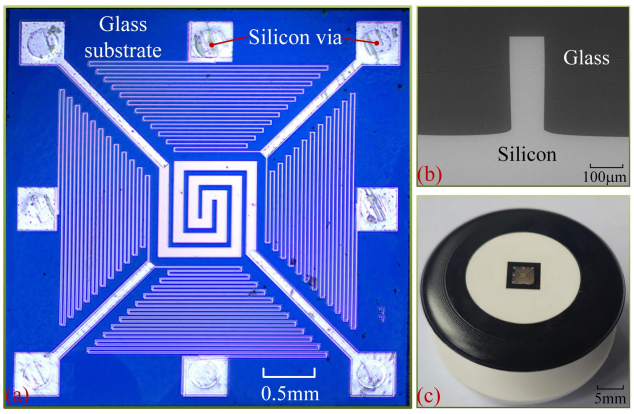

Fig. 4. Photographs of the fabricated thermal convective accelerometer. (a) Optical microscope photograph of the front side of the chip. (b) Cross-sectional SEM of the chip after glass reflow. (c) Schematic view of the packaged thermal convective accelerometer.

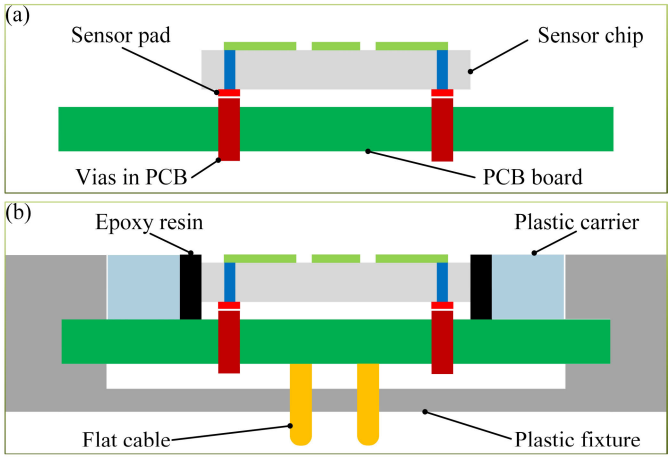

Fig. 5. Schematic cross-sectional view of the packaged thermal convective accelerometer. (a) Sensor chip bonded to the PCB. (b) Sensor chip with protection and lead wire.

The utilization of the SIG substrate significantly simplifies the packaging and integration of the sensor chip with the backend processing circuity. Fig. 5 presents the schematic of the sensor packaging process. Initially, the fabricated sensor chip is directly bonded to a PCB board. Subsequently, a 3-D-printed plastic carrier is used to encapsulate the bonded chip, and the gap between the plastic carrier and the chip is filled with epoxy resin. The plastic carrier helps ensure a relatively stable flow field on the sensor surface. Next, a 3-D-printed plastic fixture is employed to provide support for the plastic carrier. Finally, a set of flat cables can be led out from the PCB to establish further connections with the backend processing circuit.

IV. Experiment and Discussion

A. Temperature Characteristic of the Pt Thermistors

Prior to testing the performance of the thermal convective accelerometer, the electrical and thermal characteristics of the platinum thermistor fabricated on the SIG substrate were examined. The sensor chip was placed inside a temperature chamber for the measurement. Fig. 6 displays the recorded

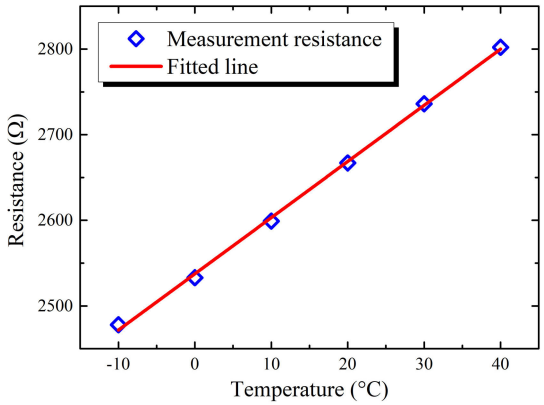

Fig. 6. Temperature coefficient test results of the platinum thermistor fabricated on SIG substrate.

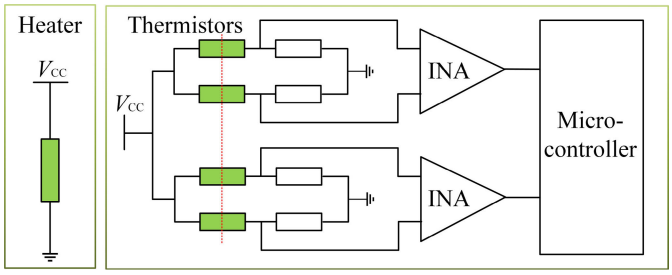

Fig. 7. Schematic of the Interface circuit used for the test of the MEMS thermal convective accelerometer.

resistance of the platinum thermistor as the chamber temperature varied from −10 °C to 40 °C in 10 °C increments. It is evident that the resistance of the platinum thermistor exhibits a linear relationship with temperature. By analyzing the resistance variation with temperature, it can be described by the equation

$$R(T) = R(T_0)(1 + \alpha(T - T_0)) \tag{3}$$

where $R(T)$ represents the resistance at temperature T, and α represents the temperature coefficient of resistance (TCR). The TCR of the platinum thermistor is calculated to be 2648 ppm/K.

B. Sensor Performance Characterization

To characterize the performance of the thermal convective accelerometer, a PCB-based interface circuit has been designed and implemented. Fig. 7 illustrates the schematic of its operating principle. The central heater of the device is supplied with a constant voltage (CV), while a Wheatstone bridge is constructed using two opposing thermistors in the x- or y-direction and two off-chip resistors. This allows for the measurement of the temperature difference between the thermistors induced by acceleration in the x- or y-direction. However, the low output voltage of the Wheatstone bridge fails to meet the sampling requirement of the microcontroller. To address this issue, instrumentation amplifiers (INAs) are adopted to amplify the output of the Wheatstone bridges. This enables the microcontroller to store the output signal of the sensor for further data analysis.

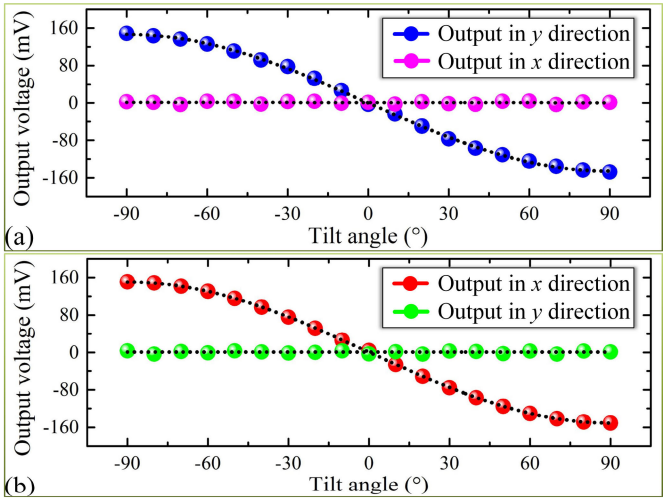

Fig. 8. Tilt angle test results of the MEMS thermal convective accelerometer. (a) Output voltage in the x- and y-directions when the sensor rotates from $-90°$ to $+90°$ around the x-axis. (b) Output voltage in the x- and y-directions when the sensor rotates from $-90°$ to $+90°$ around the y-axis.

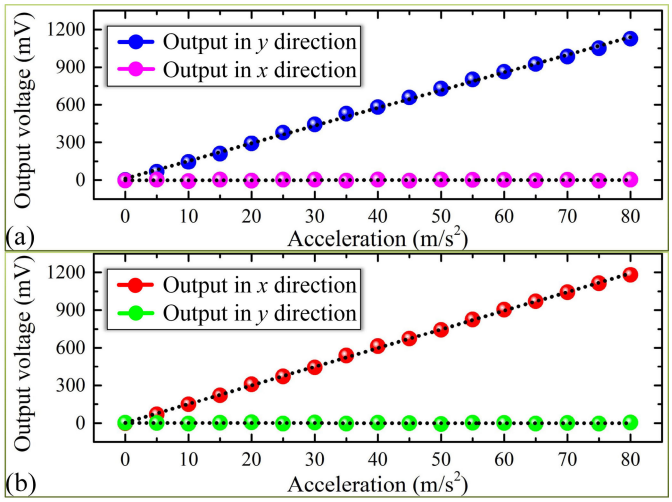

Fig. 9. Acceleration test results of the MEMS thermal convective accelerometer. (a) Output voltage in the x- and y-directions when the input acceleration is parallel to the y-direction. (b) Output voltage in the x- and y-directions when the input acceleration is parallel to the x-direction.

The packaged thermal convective accelerometer was initially placed inside a sealed box made by 3-D printing to realize encapsulation, and then, the encapsulated sensor was installed on a rotation platform to assess its response to different tilt angles. In this experiment, the heater is powered in the CV mode, with a driving power of about 110 mW. As the sensor rotates around the x-axis, the recorded output voltages correspond to the temperature difference between the two opposite thermistors located in the y- and x-directions, as shown in Fig. 8(a). Similarly, when the rotation center is the y-axis, the corresponding outputs are depicted in Fig. 8(b). It can be observed that the sensor demonstrates the capability to measure the inclination angles from $-90°$ to $90°$. The sensitivity for the y-direction and x-direction thermistors is measured as 147.86 and 150.47 mV/g, respectively. The slight difference in sensitivity between the x- and y-directions could be attributed to the manufacturing errors or the installation errors during the testing process.

The sensor was further tested under input accelerations ranging from 0 to 80 m/s^2 using a shaking table experimental setup. When the input acceleration is parallel to the y-axis direction, the output characteristics of the sensor are illustrated in Fig. 9(a), while the output voltages for the x-axis parallel input acceleration are depicted in Fig. 9(b). It is noteworthy that the sensor exhibits the capacity to measure acceleration exceeding 80 m/s^2, with the output voltage demonstrating an approximately linear variation as the input acceleration increases.

Additionally, the response time of the thermal convective accelerometer was evaluated by operating the heater in a CV mode. During this measurement, the sensor was rotated around the x-axis, causing the tilt angle to abruptly shift from $+90°$ to $-90°$. The microcontroller recorded the corresponding variation in output voltage, as illustrated in Fig. 10. The response time in this case refers to the duration needed for the output voltage to transition from 10% to 90% of its maximum value, while the tilt angle varies from $-90°$ to $+90°$. It can be observed from the data that the response time is approximately 108 ms.

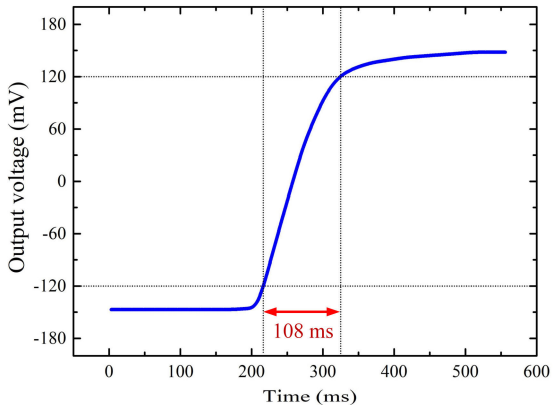

Fig. 10. Response time testing result of the thermal convective accelerometer.

V. Conclusion

A micromachined 2-D thermal convective accelerometer fabricated on an SIG substrate has been presented, fabricated, and tested. With this substrate, the heater and thermistor components of the sensor are placed on the low thermal conductivity glass bulk to reduce ineffective heat conduction and avoid the impact of stress on sensor performance commonly found in conventional silicon membrane structures. In addition, the connection between the sensor and the backend processing circuity can be achieved through the silicon pillars on the SIG substrate, significantly simplifying the integration and packaging of the sensor. This SIG substrate is manufactured by the glass reflow process, and the fabricated sensor has been experimentally evaluated. The results indicate that the sensor can measure acceleration exceeding 80 m/s^2 with an approximate linear sensitivity of about 150 mV/g. The thermal convective accelerometer presented in this article can

be utilized in areas that require high reliability and low power consumption.

REFERENCES

[1] A. Sabato, C. Niezrecki, and G. Fortino, "Wireless MEMS-based accelerometer sensor boards for structural vibration monitoring: A review," *IEEE Sensors J.*, vol. 17, no. 2, pp. 226–235, Jan. 2017.

[2] Q. Lu, Y. Wang, X. Wang, Y. Yao, X. Wang, and W. Huang, "Review of micromachined optical accelerometers: From mg to sub-μg," *Opto-Electron Adv.*, vol. 4, no. 3, pp. 20004501–20004515, Mar. 2021.

[3] C. Wang et al., "Micromachined accelerometers with sub-$\mu g/\sqrt{\text{Hz}}$ noise floor: A review," *Sensors*, vol. 20, no. 14, p. 4054, Jul. 2020.

[4] V. Narasimhan, H. Li, and M. Jianmin, "Micromachined high-g accelerometers: A review," *J. Micromech. Microeng.*, vol. 25, no. 3, Mar. 2015, Art. no. 033001.

[5] R. Mukherjee, J. Basu, P. Mandal, and P. K. Guha, "A review of micromachined thermal accelerometers," *J. Micromech. Microeng.*, vol. 27, no. 12, Dec. 2017, Art. no. 123002.

[6] F. Hosseini, M. Mehran, S. Mohajerzadeh, and O. Shoaei, "Design, analysis, simulation, and fabrication of a novel linear MEMS capacitive inclinometer," *IEEE Sensors J.*, vol. 18, no. 17, pp. 6962–6968, Sep. 2018.

[7] S. Tez, U. Aykutlu, M. M. Torunbalci, and T. Akin, "A bulk-micromachined three-axis capacitive MEMS accelerometer on a single die," *J. Microelectromech. Syst.*, vol. 24, no. 5, pp. 1264–1274, Oct. 2015.

[8] M. Daeichin, R. N. Miles, and S. Towfighian, "Large-stroke capacitive MEMS accelerometer without pull-in," *IEEE Sensors J.*, vol. 21, no. 3, pp. 3097–3106, Feb. 2021.

[9] J. Zhang, T. Wu, Y. Liu, C. Lin, and Y. Su, "Thermal stress resistance for the structure of MEMS-based silicon differential resonant accelerometer," *IEEE Sensors J.*, vol. 23, no. 9, pp. 9146–9157, May 2023.

[10] C. Zhao et al., "A resonant MEMS accelerometer with 56 ng bias stability and 98 ng/Hz$^{1/2}$ noise floor," *J. Microelectromech. Syst.*, vol. 28, no. 3, pp. 324–326, Jun. 2019.

[11] S. A. Zotov, B. R. Simon, A. A. Trusov, and A. M. Shkel, "High quality factor resonant MEMS accelerometer with continuous thermal compensation," *IEEE Sensors J.*, vol. 15, no. 9, pp. 5045–5052, Sep. 2015.

[12] X. Wang, W. Xu, H. Luo, and Y.-K. Lee, "Theoretical modeling, numerical simulations and experimental study of micro thermal convective accelerometers," *J. Microelectromech. Syst.*, vol. 28, no. 5, pp. 790–798, Oct. 2019.

[13] X. Wang, Y.-K. Lee, and W. Xu, "Sensitivity and frequency response improvement of the micro thermal convective accelerometer with structure optimization," *J. Microelectromech. Syst.*, vol. 31, no. 5, pp. 753–759, Oct. 2022.

[14] U. Park, D. Kim, J. Kim, I.-K. Moon, and C.-H. Kim, "Development of a complete dual-axis micromachined convective accelerometer with high sensitivity," in *Proc. IEEE Sensors*, Oct. 2008, pp. 670–673.

[15] R. Mukherjee, P. Mandal, and P. K. Guha, "Sensitivity improvement of a dual axis thermal accelerometer with modified cavity structure," *Microsyst. Technol.*, vol. 23, no. 12, pp. 5357–5363, Dec. 2017.

[16] R. Zhu, S. Cai, H. Ding, Y. J. Yang, and Y. Su, "A micromachined gas inertial sensor based on thermal expansion," *Sens. Actuators A, Phys.*, vol. 212, pp. 173–180, Jun. 2014.

[17] M. Wu, L. Hong, and Y. Li, "A novel optical accelerometer based on slant-ended fiber," *IEEE Sensors J.*, vol. 22, no. 12, pp. 11673–11681, Jun. 2022.

[18] B. Yan and L. Liang, "A novel fiber Bragg grating accelerometer based on parallel double flexible hinges," *IEEE Sensors J.*, vol. 20, no. 9, pp. 4713–4718, May 2020.

[19] E. Soltanian, K. Jafari, and K. Abedi, "A novel differential optical MEMS accelerometer based on intensity modulation, using an optical power splitter," *IEEE Sensors J.*, vol. 19, no. 24, pp. 12024–12030, Dec. 2019.

[20] G. K. Fedder, R. T. Howe, T.-J. King Liu, and E. P. Quevy, "Technologies for cofabricating MEMS and electronics," *Proc. IEEE*, vol. 96, no. 2, pp. 306–322, Feb. 2008.

[21] B. Arnold, "Design, manufacturing and test of a high-precision MEMS inclination sensor for navigation systems in robot-assisted surgery," *Int. J. Biomed. Sci. Eng.*, vol. 6, no. 1, p. 1, 2018.

[22] Y. Dong, P. Zwahlen, A. M. Nguyen, R. Frosio, and F. Rudolf, "Ultra-high precision MEMS accelerometer," in *Proc. 16th Int. Solid-State Sensors, Actuat. Microsystems Conf.*, Beijing, China, Jun. 2011, pp. 695–698.

[23] J. Bahari, J. D. Jones, and A. M. Leung, "Sensitivity improvement of micromachined convective accelerometers," *J. Microelectromech. Syst.*, vol. 21, no. 3, pp. 646–655, Jun. 2012.

[24] W. Xu, X. Wang, X. Zhao, and Y.-K. Lee, "Two-dimensional CMOS MEMS thermal flow sensor with high sensitivity and improved accuracy," *J. Microelectromech. Syst.*, vol. 29, no. 2, pp. 248–254, Apr. 2020.

[25] W. Xu et al., "A sub-5 mW monolithic CMOS-MEMS thermal flow sensing SoC with ±6 m/s linear range," *IEEE J. Solid-State Circuits*, early access, Sep. 22, 2023, doi: 10.1109/JSSC.2023.3314765.

[26] X. Wang, G. Lim, W. Xu, and Y.-K. Lee, "Sensitivity improvement of micro thermal convective accelerometer with structure optimization: Theoretical and experimental studies," in *Proc. IEEE SENSORS*, Oct. 2019, pp. 1–4.

[27] S.-H. Tsang, A. Haseeb Ma, K. S. Karim, A. Parameswaran, and A. M. Leung, "Monolithically fabricated polymermems 3-axis thermal accelerometers designed for automated wirebonder assembly," in *Proc. IEEE 21st Int. Conf. Micro Electro Mech. Syst.*, Tucson, AZ, USA, Jan. 2008, pp. 880–883.

[28] Y. Li and Z. Jiang, "An overview of reliability and failure mode analysis of microelectromechanical systems (MEMS)," in *Handbook of Performability Engineering*. London, U.K.: Springer, 2008, pp. 953–966.

[29] G. Harman, *Reliability and Yield Problems of Wire Bonding in Microelectronics* (International Society for Hybrid Microelectronics). New York, NY, USA: McGraw-Hill, 1993.

[30] X. Wang, W. Xu, Izhar, and Y.-K. Lee, "Theoretical and experimental study and compensation for temperature drifts of micro thermal convective accelerometer," *J. Microelectromech. Syst.*, vol. 29, no. 3, pp. 277–284, Jun. 2020.

[31] O. Behrmann, T. Lisec, and B. Gojdka, "Towards robust thermal MEMS: Demonstration of a novel approach for solid thermal isolation by substrate-level integrated porous microstructures," *Micromachines*, vol. 13, no. 8, p. 1178, Jul. 2022.

[32] J. Liu, J. Shang, J. Tang, and Q.-A. Huang, "Micromachining of Pyrex 7740 glass by silicon molding and vacuum anodic bonding," *J. Microelectromech. Syst.*, vol. 20, no. 4, pp. 909–915, Aug. 2011.

[33] Y.-Q. Zhu, B. Chen, M. Qin, J.-Q. Huang, and Q.-A. Huang, "Development of a self-packaged 2D MEMS thermal wind sensor for low power applications," *J. Micromech. Microeng.*, vol. 25, no. 8, Jul. 2015, Art. no. 085011.

[34] B. Luo, M. Ma, M.-A. Zhang, J. Shang, and C.-P. Wong, "Composite glass-silicon substrates embedded with microcomponents for MEMS system integration," *IEEE Trans. Compon., Packag., Manuf. Technol.*, vol. 9, no. 2, pp. 201–208, Feb. 2019.

[35] U. Park, B. Park, I.-K. Moon, D. Kim, and J. Kim, "Development of a dual-axis micromachined convective accelerometer with an effective heater geometry," *Microelectronic Eng.*, vol. 88, no. 3, pp. 276–281, Mar. 2011.

[36] X. B. Luo, Z. X. Li, Z. Y. Guo, and Y. J. Yang, "Thermal optimization on micromachined convective accelerometer," *Heat Mass Transf.*, vol. 38, nos. 7–8, pp. 705–712, Aug. 2002.

Yizhou Ye received the B.S. and Ph.D. degrees in electronics engineering from Southeast University, Nanjing, China, in 2013 and 2018, respectively.

He is currently an Assistant Professor with the College of Optoelectronic Engineering, Chongqing University, Chongqing, China. His current interests include micro-electromechanical system (MEMS) sensors, self-powered sensing, and flexible sensors.

Shu Wan received the B.S. and Ph.D. degrees in electronics engineering from Southeast University, Nanjing, China, in 2011 and 2019, respectively.

He is currently an Assistant Professor with the College of Optoelectronic Engineering, Chongqing University, Chongqing, China. His current research interests include flexible sensors, 2-D materials, and micro-electromechanical systems (MEMS).

Shen Li received the M.E. degree in instrument science and technology from Chongqing University, Chongqing, China, in 2021, where he is currently pursuing the Ph.D. degree with the School of Optoelectronic Engineering.

His research interests include self-powered sensing, energy harvesting, and fluid-induced vibration.

Yunhao Peng received the Ph.D. degree in instrument science and technology from Chongqing University, Chongqing, China, in 2022.

He is currently an Engineer with 26th Research Institute of China Electronics Technology Group Corporation, Chongqing. His current research interests include thermal management of electronics and RF microelectromechanical system (MEMS).

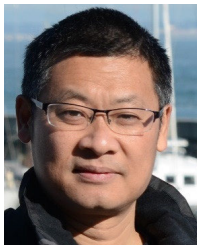

Xuefeng He (Member, IEEE) received the B.E. and M.E. degrees in mechanical engineering from the Harbin Institute of Technology, Harbin, China, in 1992 and 1995, respectively, and the Ph.D. degree in mechanical engineering from Peking University, Beijing, China, in 2005.

He is currently a Professor with Chongqing University, Chongqing, China. His research interests include energy harvesting, micro-/nanofabrication, and low-power sensors.

Ming Qin (Member, IEEE) received the B.S. degree in electrical engineering from the Wuxi Institute of Technology, Wuxi, China, in 1988, and the M.S. and Ph.D. degrees in electrical engineering from Southeast University, Nanjing, China, in 1994 and 1997, respectively.

After his graduation, he joined the Faculty Member of the Department of Electronic Engineering, Southeast University, as an Assistant Professor, where he became an Associate Professor in 1999 and a Full Professor in 2003. He was a Post-Doctoral Fellow with the Hong Kong University of Science and Technology, Hong Kong, in 1999. He was the Director of the CMOS MEMS Branch, Key Laboratory of MEMS, Ministry of Education, Southeast University. He has authored over 30 reviewed international journal articles/conference papers and holds more than 20 Chinese patents.